Chalcogenide Letters Vol. 10, No. 6, June 2013, p. 189 - 195

OPTIMIZATION OF ZINC SULFIDE (ZnS) ELECTRON AFFINITY IN COPPER INDIUM SULFIDE (CIS) BASED PHOTOVOLTAIC CELL

HADIBAH RAMLI[a*], SHARUL KAMAL ABDUL RAHIM[a],
THAREK ABD RAHIM[a], MUHAMMAD MUHAIMIN AMINUDDIN[b]
[a]Wireless Communication Center, Universiti Teknologi Malaysia, Skudai, 81310, Johor Bharu, Johor Darul Ta'zim, Malaysia
[b] IC MICROSYSTEMS Sdn. Bhd., Unit B-G-03, SME Technopreneur Centre 2, 2260
Jalan Usahawan 1, 63000 Cyberjaya, Selangor Darul Ehsan, Malaysia.

In this paper, the $CuInS_2$ thin film photovoltaic cell is presented by optimizing zinc sulfide (ZnS) electron affinity with different $CuInS_2$ carrier concentration using Silvaco TCAD. The ZnS material is suitable candidates to replace the CdS material as a buffer layer in CIS photovoltaic cell. Moreover, it is found that the performance of $CuInS_2$ thin film solar cell is relatively dependent on value ZnS electron affinity and carrier concentration of $CuInS_2$. The structure, electrical properties and optical properties is simulated in order to find the optimum ZnS electron affinity, and leading to the optimum value is obtained at χ=4.5 eV. The structure of $CuInS_2$ thin film photovoltaic cell is controlled by the χ=4.5 eV with $1x10^{16}cm^{-3}$ and $6.8x10^{17}cm^{-3}$ of $CuInS_2$ carrier concentration. The simulation shows the Jsc=25.76 mA/cm^2, Voc=1.04 V, fill factor=82.94 % and efficiency=33.59% by using $1x10^{16}cm^{-3}$ of $CuInS_2$ carrier concentration has better performance compared to the $6.8x10^{17}cm^{-3}$ of $CuInS_2$ carrier concentration.

(Received April 29, 2013; Accepted June 10, 2013)

Keywords: Thin film; Copper Indium Sulfide; Carrier concentration; Silvaco.

1. Introduction

The Cu-chalcophyrite thin film has played the role in photovoltaic technology. The typical Cu-chalcophyrite based absorber materials are $CuInS_2$, Cu(In,Ga)Se and $CuIn(S,Se)_2$. Recently, $CuInS_2$ thin film has attracted the attention due to its low cost and suitable for substituting the selenium issue to non-toxic sulfur. However, the drawback for this low cost and environment friendly $CuInS_2$ based solar cell, it gives the lowest efficiency. The highest conversion efficiency for $CuInS_2$ has reached 10.4% [1] and considerably lower than cell based on Cu(In,Ga)Se of 20.3% [2] and $CuIn(S,Se)_2$ of 12% [3]. As the potential of $CuInS_2$ based photovoltaic technology expand, a better understanding for different buffer and absorber materials is required. Extensive research has been done on zinc sulfide (ZnS) as an alternative buffer material to cadmium sulfide (CdS) in polycrystalline photovoltaic device. The ZnS is most promising material where it has a wide band gap of 3.7 eV, high index of refraction and high transmittance in visible range of solar spectrum [4-7].

In this present work, the effect of ZnS bandgap with different $CuInS_2$ absorber carrier concentrations is investigated. Section II describes the simulation details of the $CuInS_2$ photovoltaic cell. In Section III, the results from optimization of ZnS electron affinity with different $CuInS_2$ absorber carrier concentration, current density-voltage (*J-V*) characteristics and external quantum efficiency (EQE) are presented.

[*] Corresponding author:hadibahramli@yahoo.com

2. Methodology

The $CuInS_2$ solar cell consists of 0.3μm of Molybdenum layer deposited on soda lime glass (SLG) substrate and serving as a back contact for the photovoltaic cell. As the absorber photovoltaic material, $CuInS_2$ layer is deposited on top of Molybdenum with carrier concentration $1x10^{16}$ cm^{-3} with 2 μm thick. The heterojunction is then completed by deposition of 0.05 μm, $1x10^{16}$ cm^{-3} ZnS buffer layer and followed by undoped ZnO layer with thickness of 0.05 μm and $1x10^{18}$ cm^{-3} carrier concentration. The top layer or known as window layer is heavily doped by $1x10^{20}$ cm^{-3} of Al:ZnO (AZO) deposition with 0.3 μm thick as shown in Figure 1. The MgF_2 of ARC layer is deposited on top of the AZO surface to reduce the reflection of $CuInS_2$ photovoltaic cell [7].

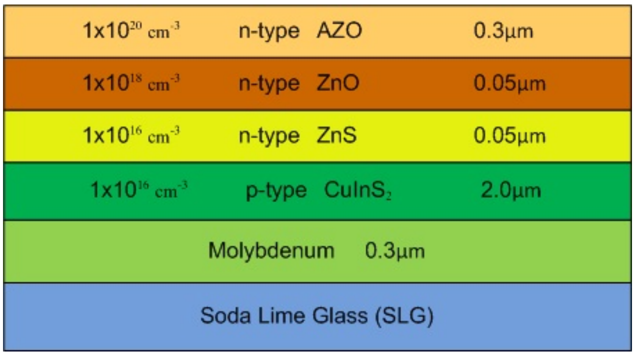

Fig. 1. Schematic diagram of $CuInS_2$ photovoltaic layer structure

The Silvaco ATLAS is used to model the $CuInS_2$ based photovoltaic device with physical parameters such as kind of materials, composition, thickness and doping concentration as shown in Figure 1 and Table 1. For the optimizing the $CuInS_2$ absorber carrier concentration and the ZnS electron affinity, the short circuit current density-voltage (*J*-*V*) characteristics, fill factor (*FF*), conversion efficiency and EQE are calculated using by default equation in Silvaco [8]. The optical properties such as the Zn (S,O) refractive index, extinction coefficient and $CuInS_2$ absorber carrier concentration are obtained from experimental value from [9-11]. The $CuInS_2$ is simulated under AM 1.5 with 1sun (100mW/cm^2) illumination.

Table 1. Physical parameters properties used in Silvaco TCAD for CIS photovoltaic cell

	AZO	ZnO	ZnS	CIS
Dielectric permittivity, ε	8.49	8.49	8.3	13.6
Energy bandgap, Eg (eV)	3.37	3.37	3.68	1.55
Electron affinity, Chi (eV)	4.5	4.5	3.9	4.58
Nc (per cc)	2.2E+18	2.2E+18	6.35E+18	2.2E+18
Nv (per cc)	1.8E+19	1.8E+19	6.03E+19	1.8E+19

3. Result and discussion

3.1 Effects of various ZnS bandgap with different carrier concentrations of CIS absorber layer

The optimization of ZnS electron affinity is investigated in this numerical simulation. The values of electron affinity of ZnS are varied from 3.9 eV to 5.2 eV with CIS electron affinity is remaining constant at 4.7 eV. Figure 2 shows the short current density, open circuit voltage, fill factor and efficiency as the function of the electron affinity in $CuInS_2$ photovoltaic cell. The performance of $CuInS_2$ photovoltaic cell is strongly dependent on ZnS electron affinity and different carrier concentration in the $CuInS_2$ absorber layer. Hence, the current density for $CuInS_2$ can be maximized by varying the value of electron affinity in ZnS buffer layer.

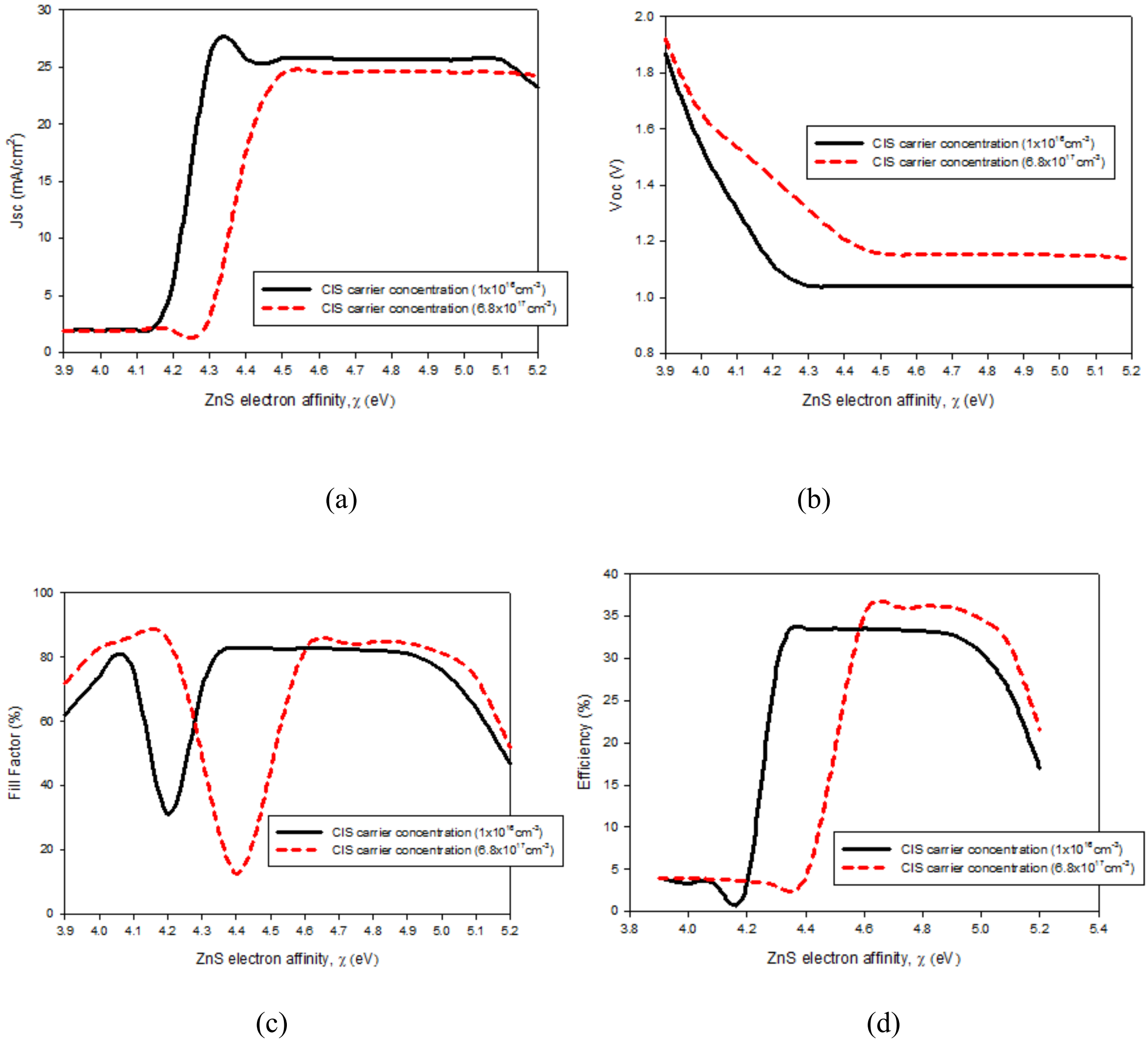

Fig. 2. Performance comparison of $CuInS_2$ photovoltaic cell with different absorber layer concentration.

The changes of performance of $CuInS_2$ can be seen in Figure 2 (a) as the electron affinity is increase. At χ=3.9 eV, the Jsc=1.88 mA/cm^2 is obtained for both different CIS absorber carrier concentration. As the electron affinity is increase to 4.4 eV, the Jsc=25.77 mA/cm^2. It is noted that Jsc is gradually decreased from Jsc=25.76 mA/cm^2 to Jsc=23.18 mA/cm^2, as the electron affinity is increase from χ=4.5 eV to χ=5.2 eV as shown in Jsc graph in Figure 2 (a). For the concentration 6.8x10^{17}cm^{-3} (red line), the Jsc value increase as the electron affinity increase from χ=3.9 eV to χ=4.6 eV. At the point χ=4.6 eV, the Jsc=24.60 mA/cm^2 and it is continuously decreased up to χ=5.2 eV. The value for Voc of the $CuInS_2$ photovoltaic cell from Figure 2 (b) is exponentially decreased from Voc=1.88 V at the χ=3.9 eV to χ=5.2 eV where the Voc is1.04 V for lower concentration. As the CIS carrier concentration is 6.8x10^{17}cm^{-3}, it is noted the value of Voc is increase by 0.05 V. The Voc graph is exponentially decrease, same with the Voc graph at $1x10^{16}cm^{-3}$ carrier concentration.

By optimizing the electron affinity of ZnS at CIS carrier concentration $1x10^{16}cm^{-3}$, the fill factor, FF can be obtained from Figure 2 (c). At χ=3.9 the FF is 62.14% and increase by 11.86 % with χ=4.0 eV. As the electron affinity is increase up χ=4.2, the FF is drastically dropped to 30.91 %. In the case χ=4.3 eV to χ=4.8 eV, the FF rapidly increase from 70.39 % to 82.16 %. The decrement value of FF is 34.42%, as the electron affinity goes up from χ=4.9 eV to χ=5.2 eV. For CIS carrier concentration $6.8x10^{17}cm^{-3}$, it can be seen the graph is shifted to the right from χ=4.2 eV to χ=4.4 eV. At the point χ=4.4 eV, the FF value is 12.55 % which smaller than 30.91 % at χ=4.4 eV for CIS carrier concentration at $1x10^{16}cm^{-3}$.

The efficiency for CIS concentration for $1x10^{16}cm^{-3}$ and $6.8x10^{17}cm^{-3}$ can be identified as the ZnS electron affinity is varied. As the electron affinity is increase from χ=3.9 eV to χ=4.1 eV, the efficiency is decreased by 0.99% and dropped to 3.23% at χ=4.2eV. The efficiency is drastically increase up from 28.72% at χ=4.3eV to 33.59% at χ=4.5eV. It can seen that at χ=4.5eV, the smaller conduction band offset ZnS/CIS heterojunction the better its power conversion efficiency. By increasing the electron χ=4.6 to χ=5.2 eV, the percentage of efficiency shows the dropping behavior from 33.95% to 16.99% as shown in Fig.2. For CIS carrier concentration $6.8x10^{17}cm^{-3}$, the shows the increment of efficiency behavior from χ=3.9 eV to χ=4.2 eV. The percentage efficiency at χ=4.3 eV is 4.01%, and continuously increase its efficiency 36.29% at χ=4.7 eV. From Fig.2, the dropping behavior of percentage efficiency from 36.13% to 21.58% are related to the increasing of electron affinity at χ=4.8 eV up to χ=5.2 eV. In Table 3, it is summarized the performance of $CuInS_2$ as a function of ZnS electron affinity (attached in last page).

3.2 Comparison on two CIS carrier concentration with optimum ZnS electron affinity, χ=4.5eV

Fig. 3 shows the fourth quadrant current density versus voltage (*J-V*) curve of the $CuInS_2$ photovoltaic cell under Air Mass 1.5 (AM 1.5) at 1 sun ($100mW/cm^2$) intensity. The χ=4.5eV is chosen as the optimum value due to ΔE=0.2 eV conduction band offset and have good percentage of efficiency. From Fig.3, the *J-V* curve gives the Jsc value at 25.76 mA/cm^2 and 24.39 mA/cm^2 for CIS carrier concentration at $1x10^{16}cm^{-3}$ It is noted that the changes of the *J-V* curves are strongly related to the CIS carrier concentration. By using the two different carrier concentration, the percentage of efficiency is dropping from 19.07% to 33.59%. These performance parameters of $CuInS_2$ is comparable with the reported in [1] as shown in Table 2.

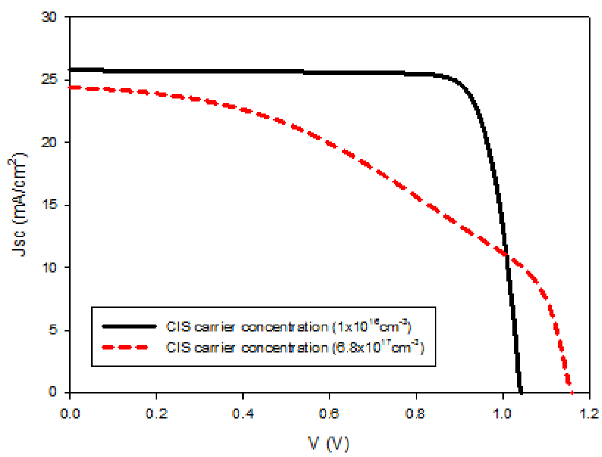

Fig. 3. I-V curve at different CIS carrier concentration with χ=4.5 eV

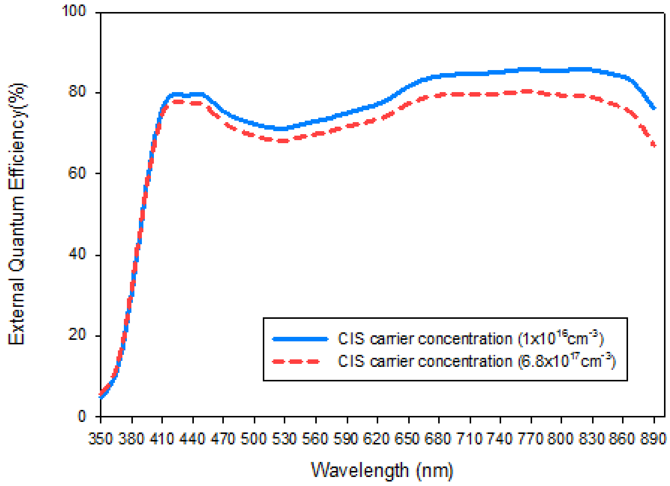

Fig. 4: EQE for $CuInS_2$ solar cell as a function of wavelength under χ=4.5 eV in ZnS layer at different carrier concentration of $CuInS_2$.

The result of external quantum efficiency (EQE) of $CuInS_2$ photovoltaic solar cell is plotted in Fig.4. In the wavelength range of 440nm-890nm, the CIS carrier concentration $1x10^{16}cm^{-3}$ exhibit a higher EQE compared than CIS carrier concentration $6.8x10^{17}cm^{-3}$. The highly transparency of ZnS buffer layer has leads the absorption at shorter wavelength range from 350nm to 440nm and decrease the short circuit current density 1 mA/cm^2 corresponding to higher $CuInS_2$ carrier concentration.

Table 2 Parameters of the optimized carrier concentration in absorber layer with electron affinity, χ=4.5eV

Solar cells	Jsc (mA/cm^2)	Voc (V)	FF (%)	Efficiency (%)
Reference model [1]	24.50	0.70	65.80	10.4
CIS optimized at absorber layer ($1x10^{16}cm^{-3}$)	25.76	1.04	82.94	33.59
CIS optimized at absorber layer ($6.8x10^{17}cm^{-3}$)	24.39	1.15	44.82	19.07

The comparisons are given in Table 2 and Fig.4. It is clearly seen that to improvised the performance of $CuInS_2$ thin film photovoltaic cell with different $CuInS_2$ carrier concentration, EQE, Jsc, Voc, FF and efficiency has been achieved. Since the operation of photovoltaic cell includes the process of recombination, conduction band offset, and photon absorption, thus many parameters needs to take into account in order to improve the performance of solar cell especially in term of simulation. Further investigation is required in the next simulation especially in material defects, surface recombination and valence band offset.

Table 3:Parameters of the $CuInS_2$ photovoltaic cell with different $CuInS_2$ carrier concentration. Here Jsc is short current density, Voc is open circuit voltage, FF is fill factor

CIS concentration (cm^{-3})	ZnS Electron Affinity, χ (eV)	Jsc (mA/cm^2)	Voc (V)	FF (%)	Efficiency (%)
$1x10^{16}$	3.9	1.88	1.87	62.14	3.95
	4.0	1.88	1.54	74.00	3.24
	4.1	1.97	1.31	75.67	2.96
	4.2	6.18	1.12	30.91	3.23
	4.3	25.85	1.04	70.39	28.72
	4.4	25.77	1.04	82.79	33.54
	4.5	25.76	1.04	82.74	33.59
	4.6	25.75	1.04	82.84	33.55
	4.7	25.74	1.04	82.60	33.45
	4.8	25.72	1.04	82.16	33.25
	4.9	25.70	1.04	81.17	32.84
	5.0	25.68	1.04	76.06	30.75
	5.1	25.64	1.04	64.28	25.92
	5.2	23.18	1.04	46.75	16.99
$6.8x10^{17}$	3.9	1.88	1.92	71.76	3.92
	4.0	1.88	1.66	82.81	3.91
	4.1	1.88	1.54	86.68	3.79
	4.2	1.91	1.42	85.52	3.51
	4.3	2.99	1.31	49.35	2.93
	4.4	17.54	1.21	12.55	4.01
	4.5	24.39	1.16	44.82	19.07
	4.6	24.60	1.15	81.93	35.07
	4.7	24.60	1.15	84.80	36.29
	4.8	24.57	1.15	84.75	36.25
	4.9	24.58	1.15	84.52	36.13
	5.0	24.56	1.15	81.28	34.70
	5.1	24.54	1.15	73.70	31.37
	5.2	24.27	1.14	51.73	21.58

4. Conclusion

The $CuInS_2$ thin film photovoltaic cell is designed by optimizing the conduction band offset of ZnS /CIS heterojunction with two difference carrier concentration. It is found that electron affinity, χ=4.5 eV is optimum value with ΔE=0.2 eV of conduction band offset. Our results demonstrate the performance of the $CuInS_2$ is improved from 19.07% to 33.59% under AM 1.5 for the CIS carrier concentration $1x10^{16}cm^{-3}$ under $100mW/cm^2$ illumination. Based on by the previous experimental value which added in new design, we observed that the performance results of $CuInS_2$ baseline model can be comparable with our $CuInS_2$ design and hence may gives a better understanding behind the physics behavior especially in $CuInS_2$ thin film photovoltaic cell.

Acknowledgement

This work is supported by the National Flagship Research University (RU) Grant funded by the Ministry of Science, Technology and Innovation (MOSTI) (Q.J130000.2423.00G35). The ICMicrosystem Sdn. Bhd. Has also contributed to the device design and provides the technology support.

References

[1] A. Ennaoui, M. Bär, J. Klaer, T. Kropp, Progress in Photovoltaics: Research and Applications, **14**, 499 (2006).

[2] P. Jackson, D. Hariskos, E. Lotter et al., Progress in Photovoltaics: Research and Applications, **19**(7), 894 (2011).

[3] W. Liu, D. B. Mitzi, M. Yuan et al., Chemistry of Materials,**22**, 1010 (2009).

[4] L. Zhou, Y. Xue, L.I. Jianfeng, Journal of Environmental Scienes, **21**, 76 (2009).

[5] Y. Z. Zhao, S. C. Eou, J. K. Sang, Materials Chemi stry and Physics, **135**, 287 (2012).

[6] U. Gangopadhyay, K. Kim, D. Manglaraj, Applied Surface Science, **230**, 364 (2004).

[7] K. Lee, J. D. Zimmerman, X. Xiao, K. Sun and S. R. Forrest, Journal Of Applied Physics, **111**, 0335271 (2012).

[8] Silvaco Atlas's User Manual, Silvaco Inc, 2012.

[9] M. Y. Nadeem, W. Ahmed, Turkish Journal of Physics, **24**, 651 (2000).

[10] D. A. Miller, G. R. Kowach, "Optical Properties of Zinc Oxide and Strontium Titanate Thin Film s by Reflectometry and Ellipsometry," University of New York, pp.16, 2007.

[11] H. H. Yang, G. C. Park, Transactions on Electrical and Electronic Materials, **11**, 73 (2010).